iScience, Volume *25*

Supplemental information

Cell cycle defects underlie childhood-onset cardiomyopathy associated with Noonan syndrome

Anna B. Meier, Sarala Raj Murthi, Hilansi Rawat, Christopher N. Toepfer, Gianluca Santamaria, Manuel Schmid, Elisa Mastantuono, Thomas Schwarzmayr, Riccardo Berutti, Julie Cleuziou, Peter Ewert, Agnes Görlach, Karin Klingel, Karl-Ludwig Laugwitz, Christine E. Seidman, Jonathan G. Seidman, Alessandra Moretti, and Cordula M. Wolf

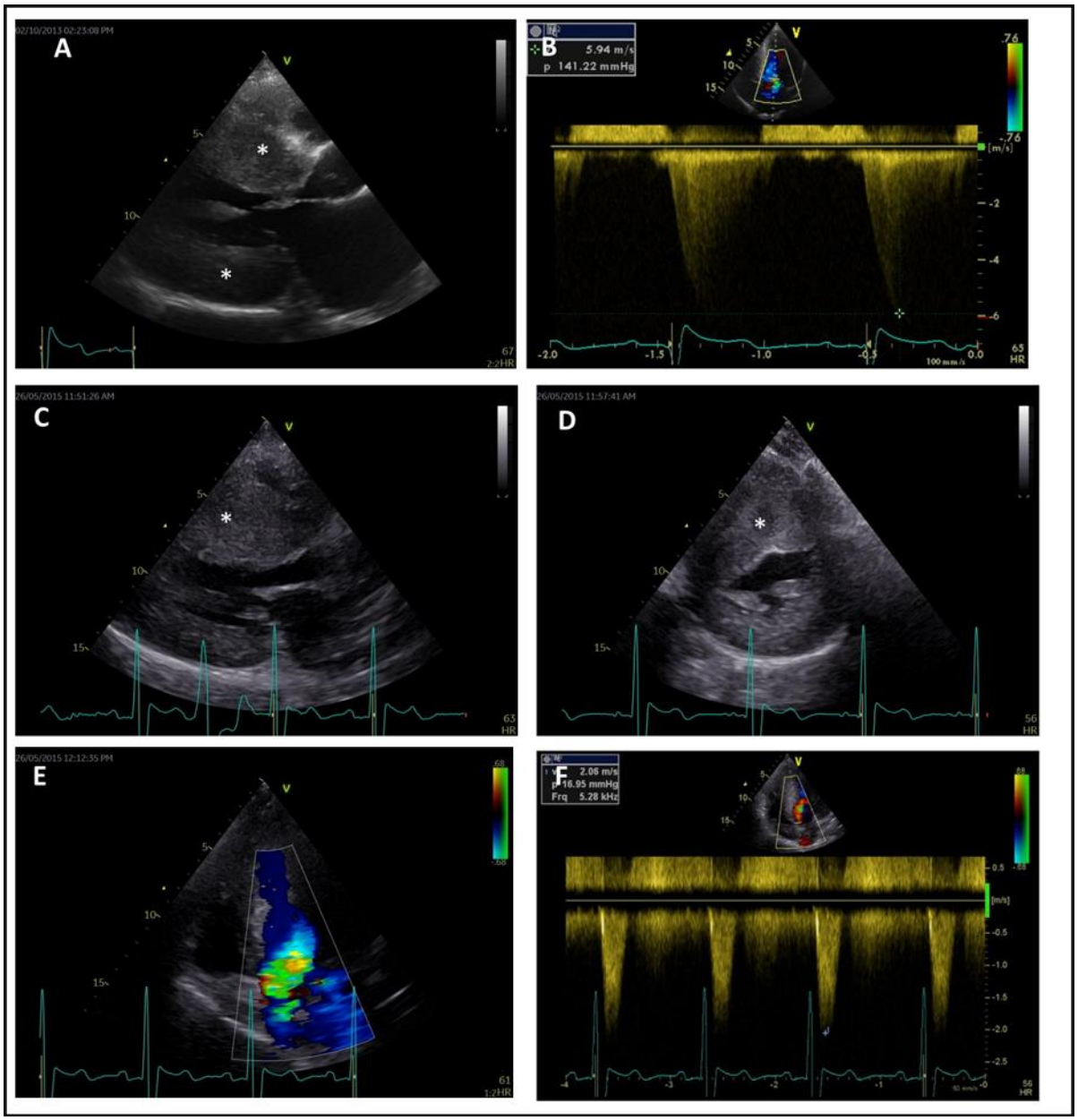

Figure S1. Echocardiographic images of patient 1, Related to Figure 1. Transthoracic echocardiographic imaging of patient 1 (Noonan syndrome, *RAF1*, male, 165 months of age) at the time of admission to the hospital for surgical left ventricular outflow tract resection (panel A and B), and at the time of follow-up (184 months of age, panel C, D, E and F). Depicted are the parasternal long axis view (panel A and C), parasternal short axis view (panel D), and the apical 5-chamber view (panel B and E) with color Doppler (panel E) and continuous wave (CW) Doppler (panel B and D) imaging. There is severe myocardial thickening (*), the peak gradient over the left ventricular outflow tract measures 130 mmHg before resection of the left ventricular outflow tract (panel B). There is no obstruction of the left ventricular outflow tract at the time of follow-up (panel F).

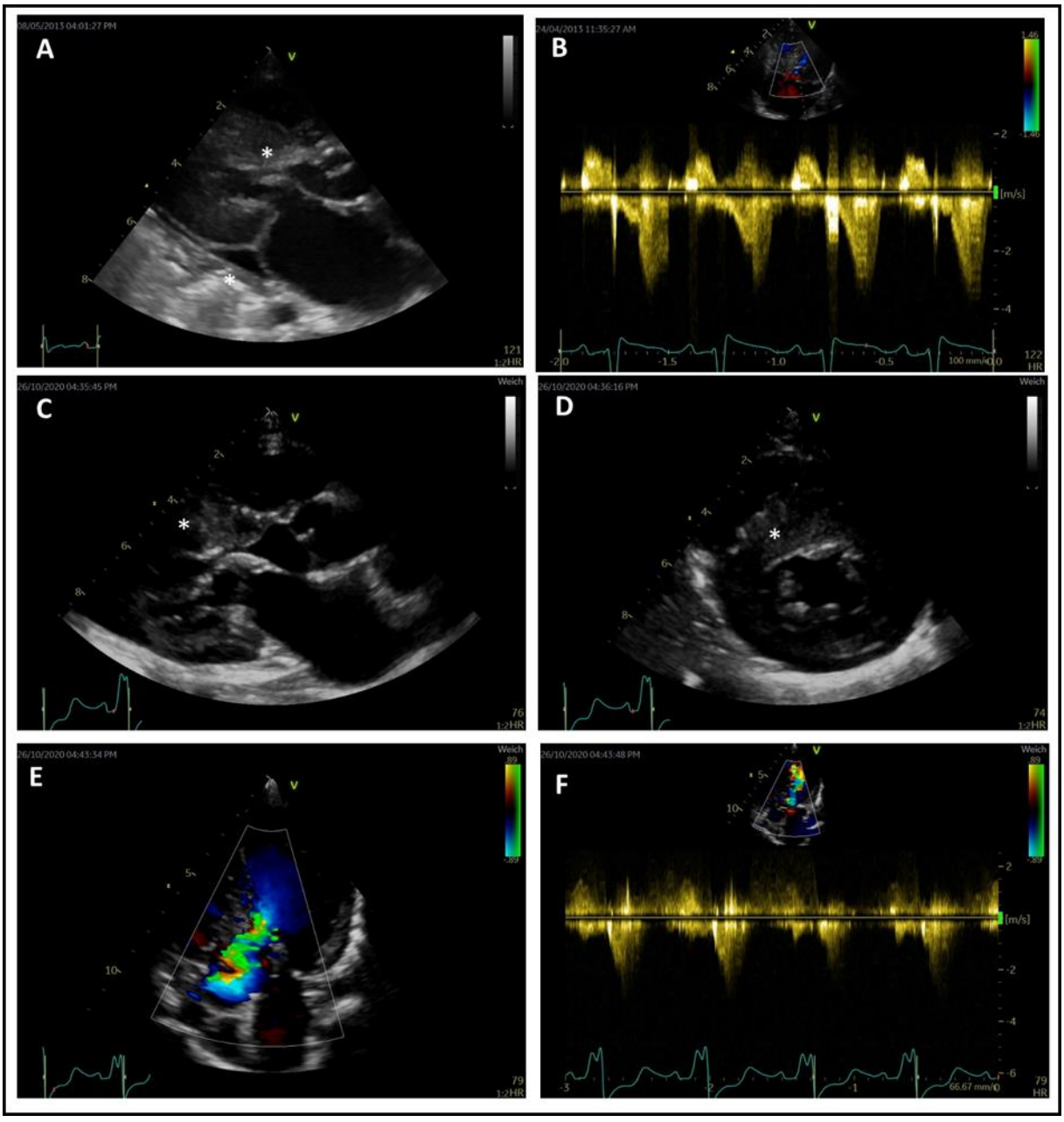

Figure S2. Echocardiographic images of patient 2, Related to Figure 1. Transthoracic echocardiographic imaging of patient 2 (Noonan syndrome, *RAF1*, female, 12 months of age) at the time of admission to the hospital for surgical left ventricular outflow tract resection (panel A and B), and at the time of follow-up (101 months of age, panel C, D, E and F). Depicted are the parasternal long axis view (panel A and C), parasternal short axis view (panel D), and the apical 5-chamber view (panel B and E) with color Doppler (panel E) and continuous wave (CW) Doppler (panel B and D) imaging. There is severe myocardial thickening (*), the peak gradient over the left ventricular outflow tract measures 75 mmHg before resection of the left ventricular outflow tract (panel B), and 40 mmHg at the time of follow-up (panel F).

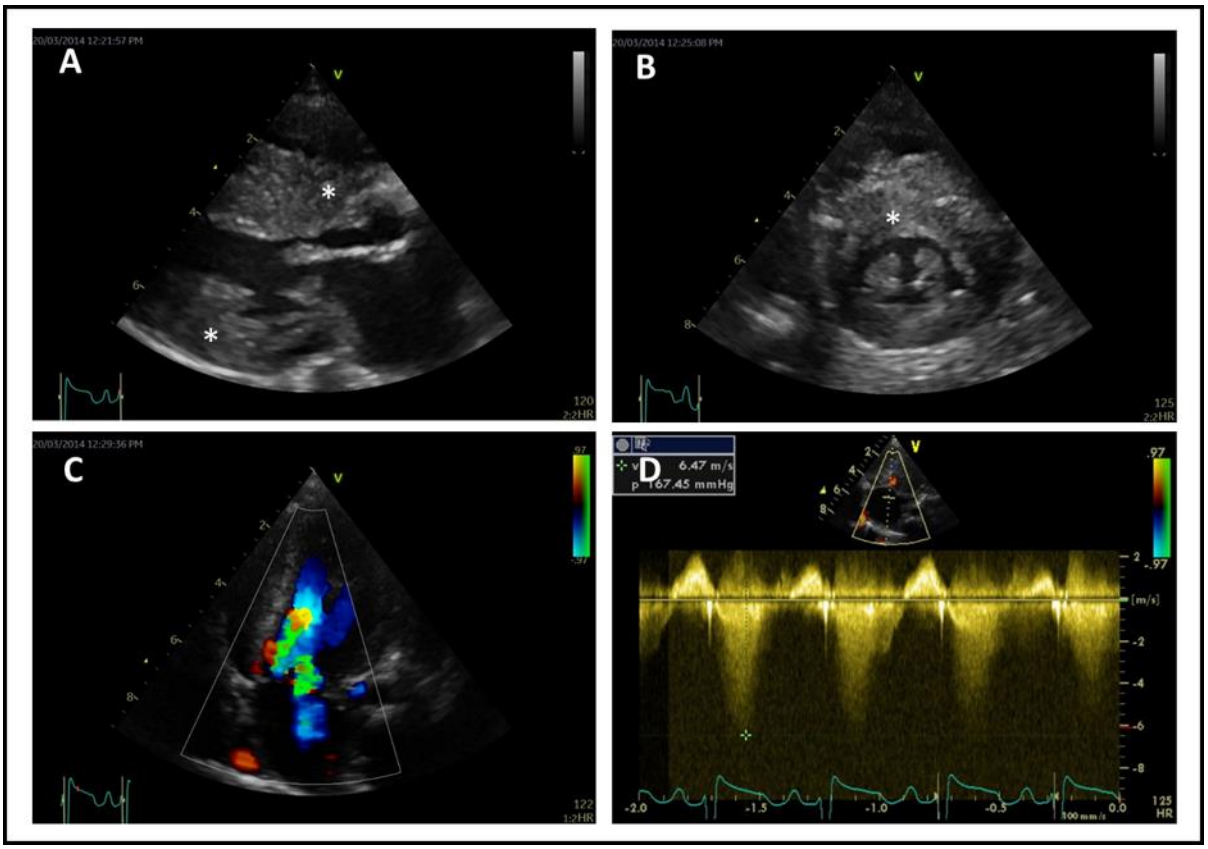

Figure S3. Echocardiographic images of patient 3, Related to Figure 1. Transthoracic echocardiographic imaging of patient 3 (Noonan syndrome, *RAF1*, male, 11 months of age) at the time of admission to the hospital for surgical left ventricular outflow tract resection. Depicted are the parasternal long axis view (panel A), parasternal short axis view (panel B), and the apical 5-chamber view (panel C and D) with color Doppler (panel C) and continuous wave (CW) Doppler (panel D) imaging. There is severe myocardial thickening (*), the peak gradient over the left ventricular outflow tract measures 130 mmHg.

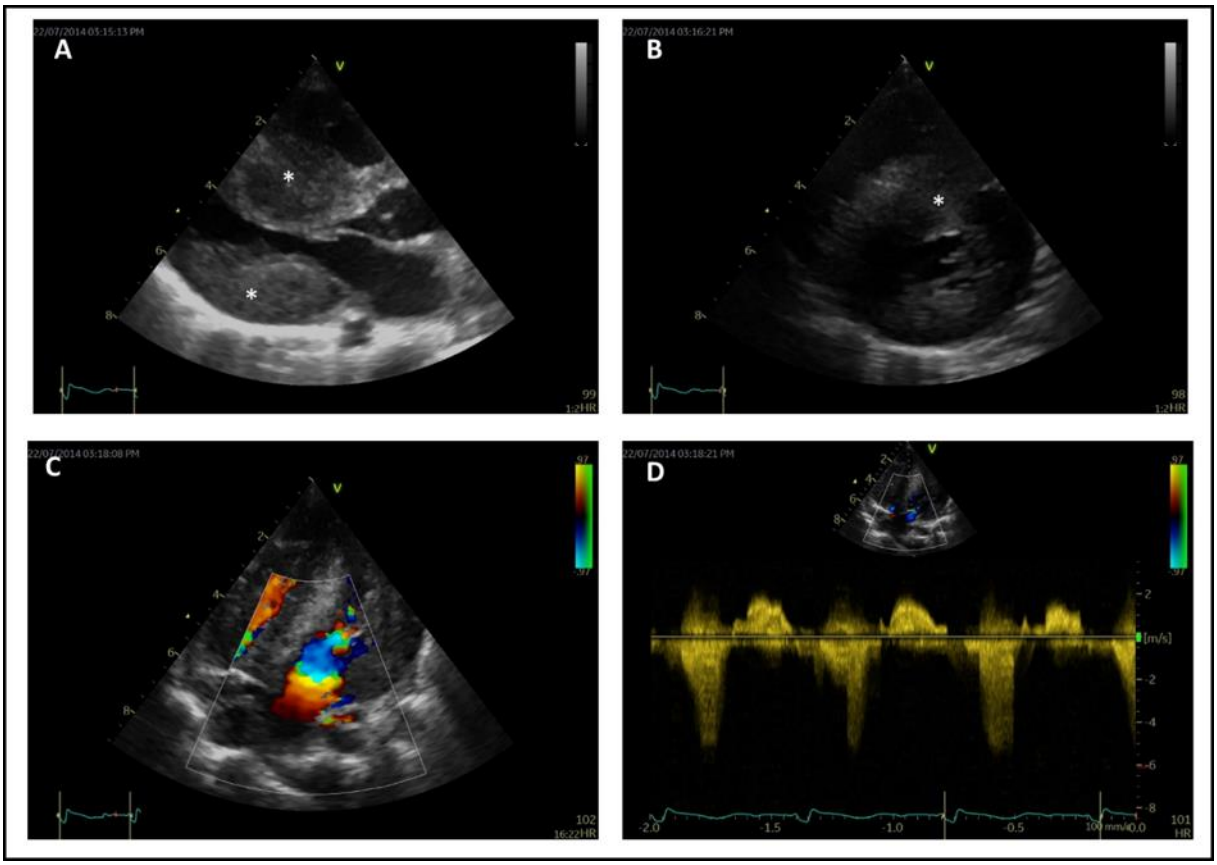

Figure S4. Echocardiographic images of patient 4, Related to Figure 1. Transthoracic echocardiographic imaging of patient 4 (Noonan syndrome, *PTPN11*, female, age 13 months) at the time of admission to the hospital for surgical left ventricular outflow tract resection. Depicted are the parasternal long axis view (panel A), parasternal short axis view (panel B), and the apical 5-chamber view (panel C and D) with color Doppler (panel C) and continuous wave (CW) Doppler (panel D) imaging. There is severe myocardial thickening (*), the peak gradient over the left ventricular outflow tract measures 72 mmHg.

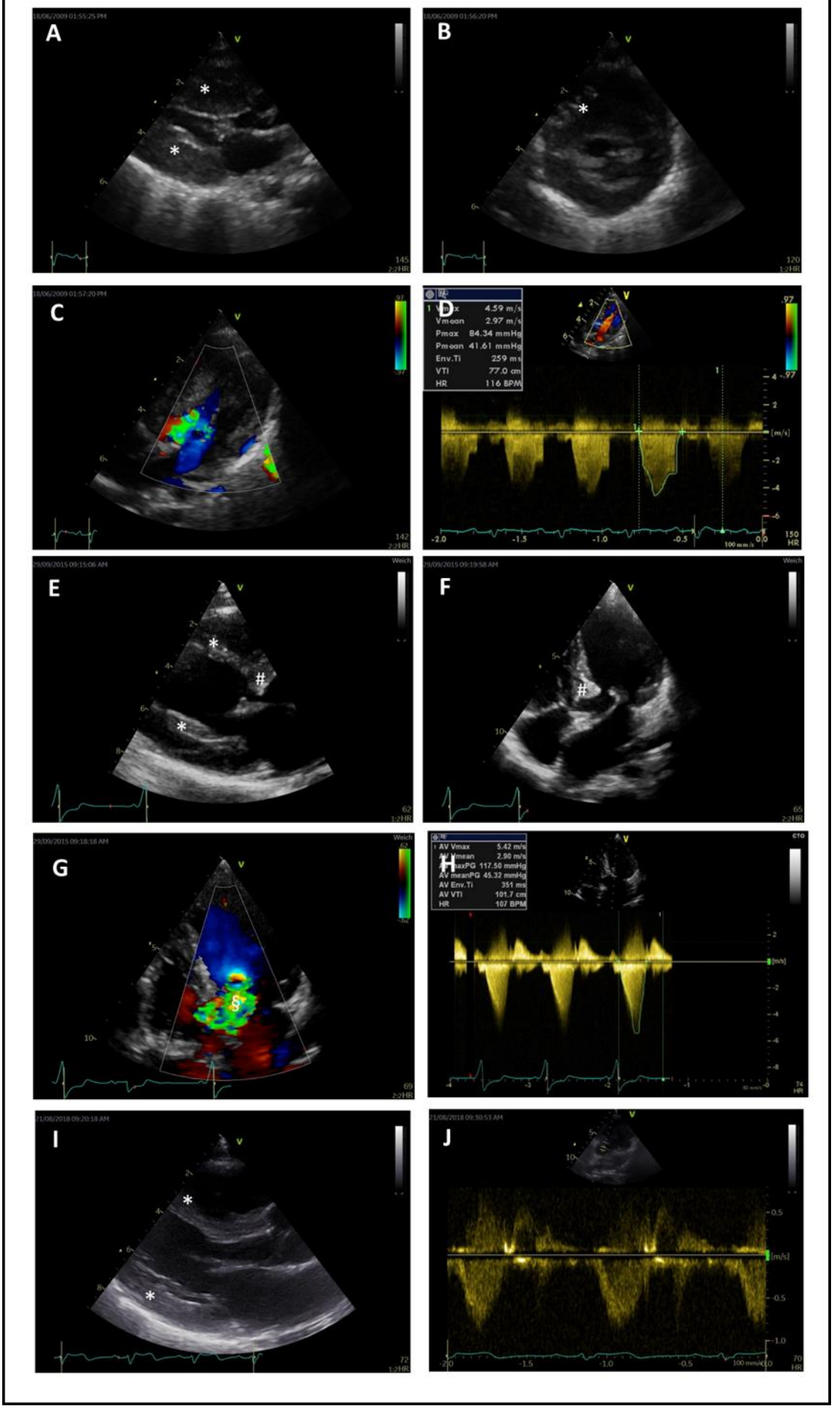
A
B
C
D
Vmax 4.59 m/s
Vmean 2.97 m/s
Pmax 84.34 mmHg
Pmean 41.61 mmHg
Env.Ti 259 ms
VTI 77.0 cm
HR 116 BPM
E
F
G
H
AV Vmax 5.42 m/s
AV Vmean 2.96 m/s
AV maxPG 117.50 mmHg
AV meanPG 45.32 mmHg
AV Env.Ti 351 ms
AV VTI 101.7 cm
HR 107 BPM
I
J

Figure S5. Echocardiographic images of patient 5, Related to Figure 1. Transthoracic echocardiographic imaging of patient 5 (Noonan syndrome, *PTPN11*, male, 2 months of age) at the time of admission to the hospital for surgical left ventricular outflow tract resection (panel A – D). Depicted are the parasternal long axis view (panel A), parasternal short axis view (panel B), and the apical 5-chamber view (panel C and D) with color Doppler (panel C) and continuous wave (CW) Doppler (panel D) imaging. There is severe myocardial thickening (*), the peak gradient over the left ventricular outflow tract measures 85 mmHg. At 76 months of age (panel E – H), myocardial hypertrophy was much less pronounced (* in panel E), but there was a remaining spur in the left ventricular outflow tract below the aortic valve (# in panel F) causing a localized obstruction (§ in panel G) with a gradient of up to 118 mmHg (panel H). The patient underwent a second surgical resection of this left ventricular outflow tract spur at this point. Follow-up at 109 months of age showed enddiastolic myocardial wall thickness z-score within the normal range and no outflow tract obstruction (panel I and J).

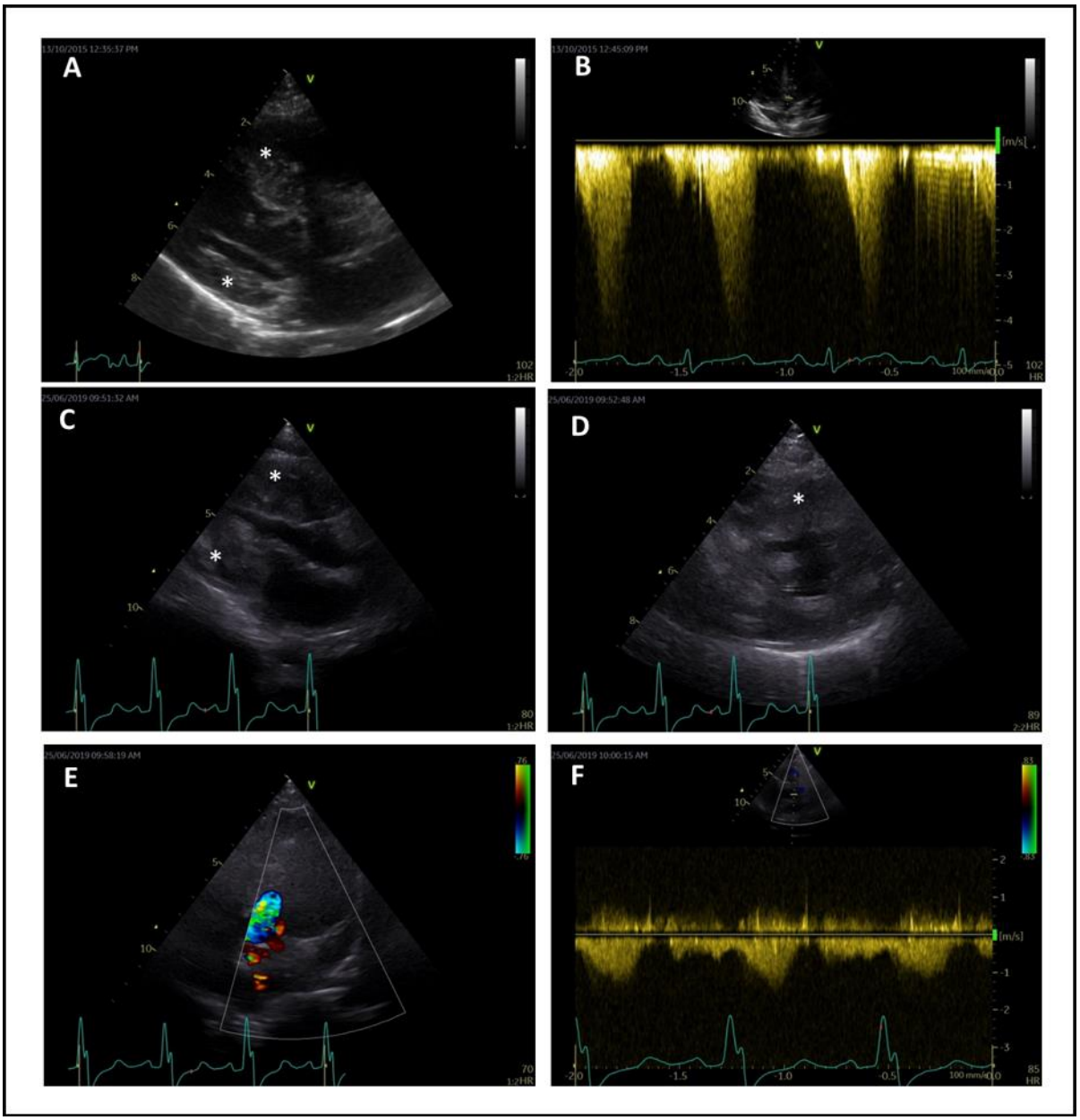

Figure S6. Echocardiographic images of patient 6, Related to Figure 1. Transthoracic echocardiographic imaging of patient 6 (Noonan syndrome, *RAF1*, female, 34 months of age) at the time of admission to the hospital for surgical left ventricular outflow tract resection (panel A and B), and at the time of follow-up (78 months of age, panel C, D, E and F). Depicted are the parasternal long axis view (panel A and C), parasternal short axis view (panel D), and the apical 5-chamber view (panel B and E) with color Doppler (panel E) and continuous wave (CW) Doppler (panel B and D) imaging. There is severe myocardial thickening (*), the peak gradient over the left ventricular outflow tract measures 92 mmHg before resection of the left ventricular outflow tract (panel B). There is no obstruction of the left ventricular outflow tract at the time of follow-up (panel F).

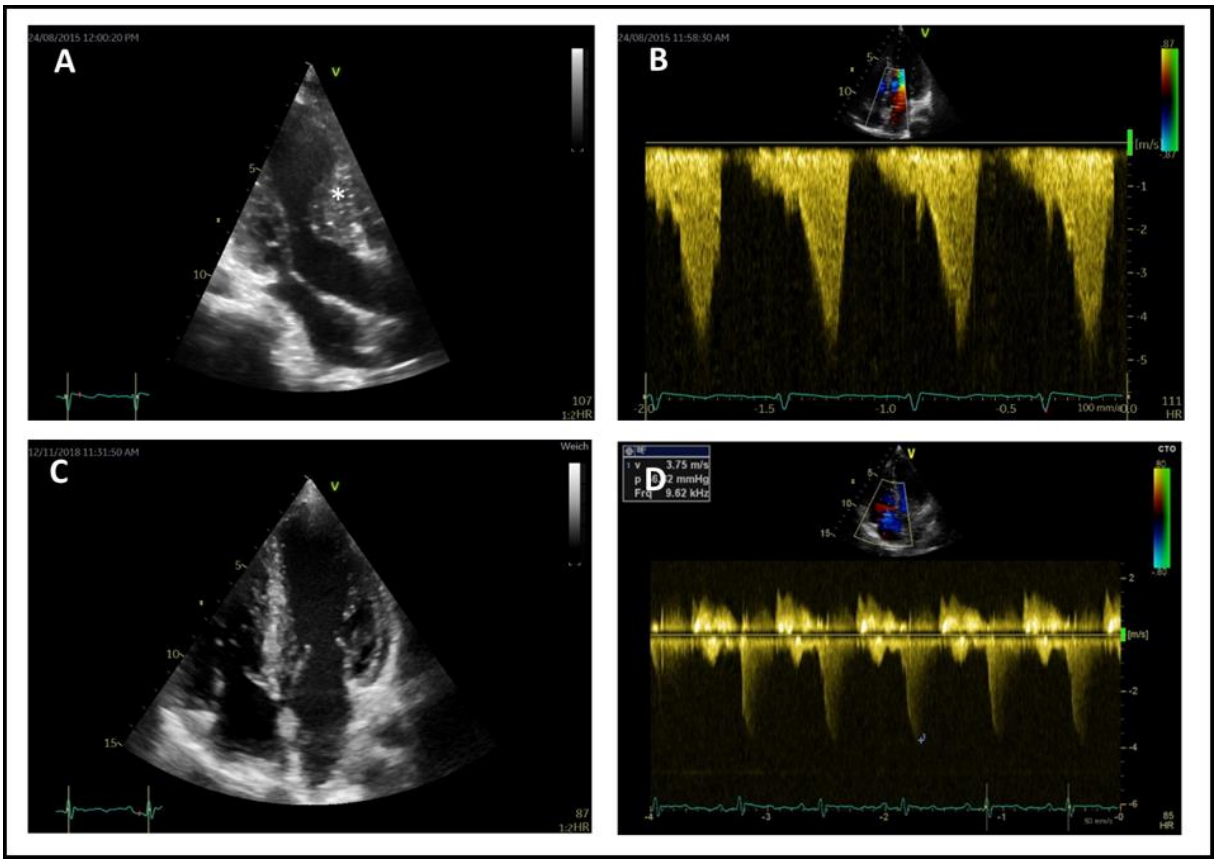

Figure S7. Echocardiographic images of patient 7, Related to Figure 1. Transthoracic echocardiographic imaging of patient 7 (Noonan syndrome, *PTPN11*, male, 182 months of age) at the time of admission to the hospital for surgical left ventricular outflow tract resection (panel A and B), and at the time of follow-up (220 months of age, panel C and D). Depicted are the apical 3-chamber view (panel A), the apical 4-chamber view (panel C), and the apical 5-chamber view with continuous wave (CW) Doppler (panel B and D) imaging. There is severe myocardial thickening (*), the peak gradient over the left ventricular outflow tract measures 105 mmHg before resection of the left ventricular outflow tract (panel B). There is reduced obstruction of the left ventricular outflow tract at the time of follow-up (panel D).

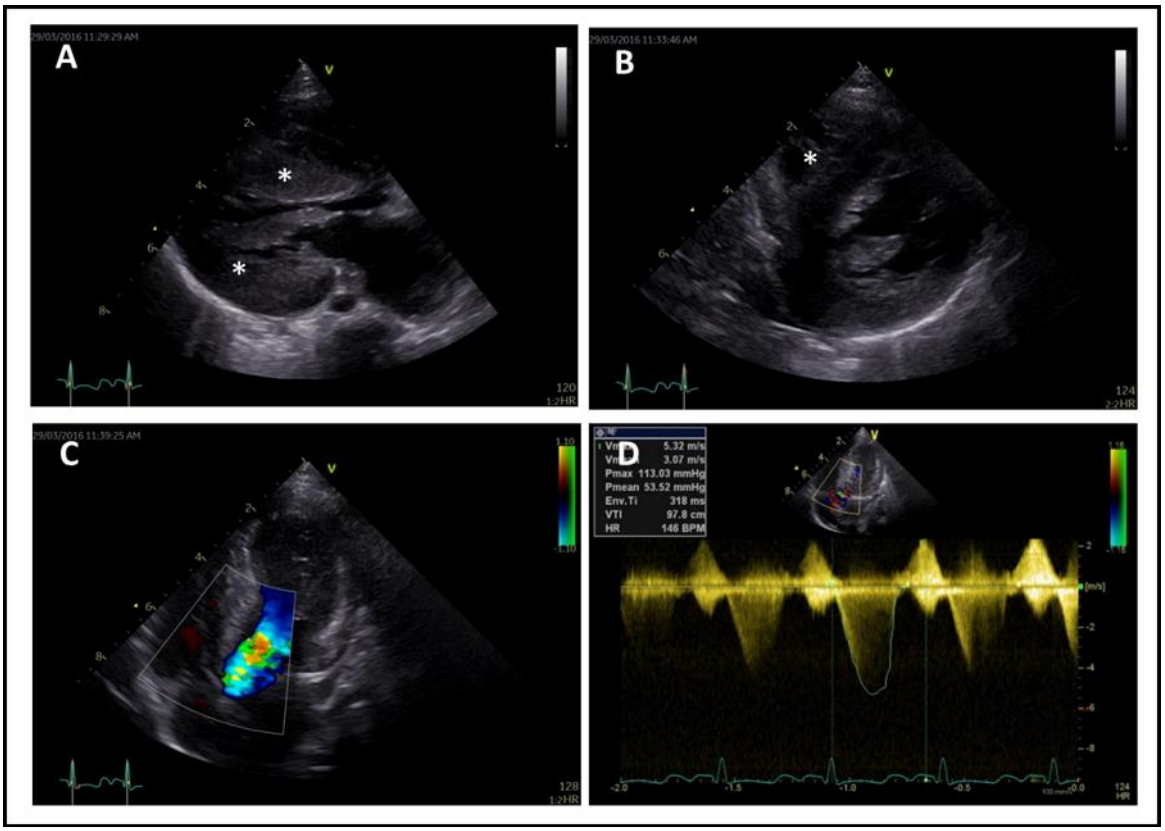

Figure S8. Echocardiographic images of patient 8, Related to Figure 1. Transthoracic echocardiographic imaging of patient 8 (Noonan syndrome, *RAF1*, female, 12 months of age) at the time of admission to the hospital for surgical left ventricular outflow tract resection. Depicted are the parasternal long axis view (panel A), parasternal short axis view (panel B), and the apical 5-chamber view (panel C and D) with color Doppler (panel C) and continuous wave (CW) Doppler (panel D) imaging. There is severe myocardial thickening (*), the peak gradient over the left ventricular outflow tract measures 140 mmHg.

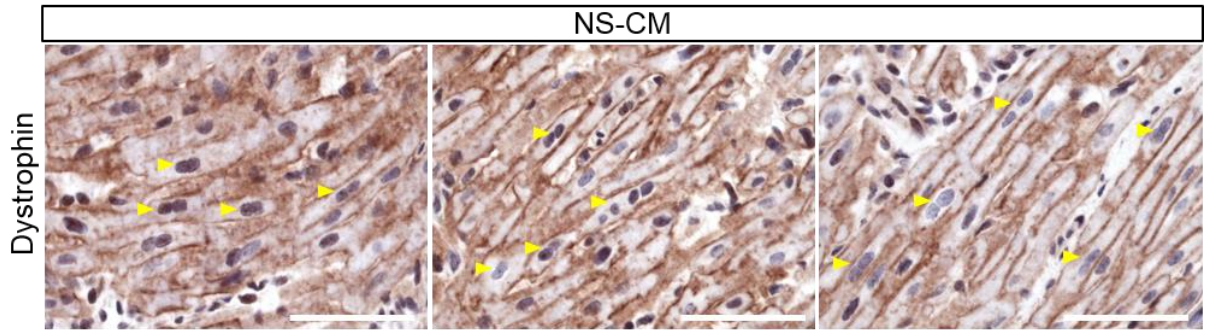

Figure S9. Histological analysis of NS-CM patients LV myocardial tissue, Related to Figure 1. Representative images of LV myocardial tissue from NS-CM patients stained for dystrophin to mark the plasma membrane of cardiomyocytes. Yellow arrowheads indicate examples of multinucleation. Scale bars = 25 µm.

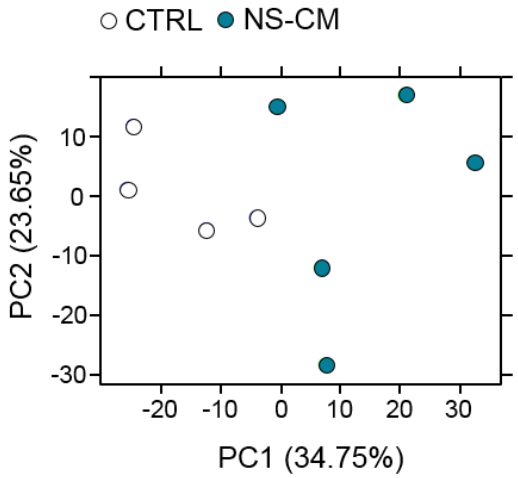

Figure S10. Principal component analysis of NS-CM patients left ventricular myocardial tissue, Related to Figure 2. Principal component analysis of RNA sequencing data of left ventricular (LV) myocardial tissue collected during septal myectomy from patients with Noonan syndrome-associated hypertrophic cardiomyopathy (NS-CM; mutated *PTPN11* N = 2 patients; mutated *RAF1* N = 3) or during ventricular septal defect repair surgery from otherwise healthy pediatric patients (CTRL; N = 4). PC = principal component.

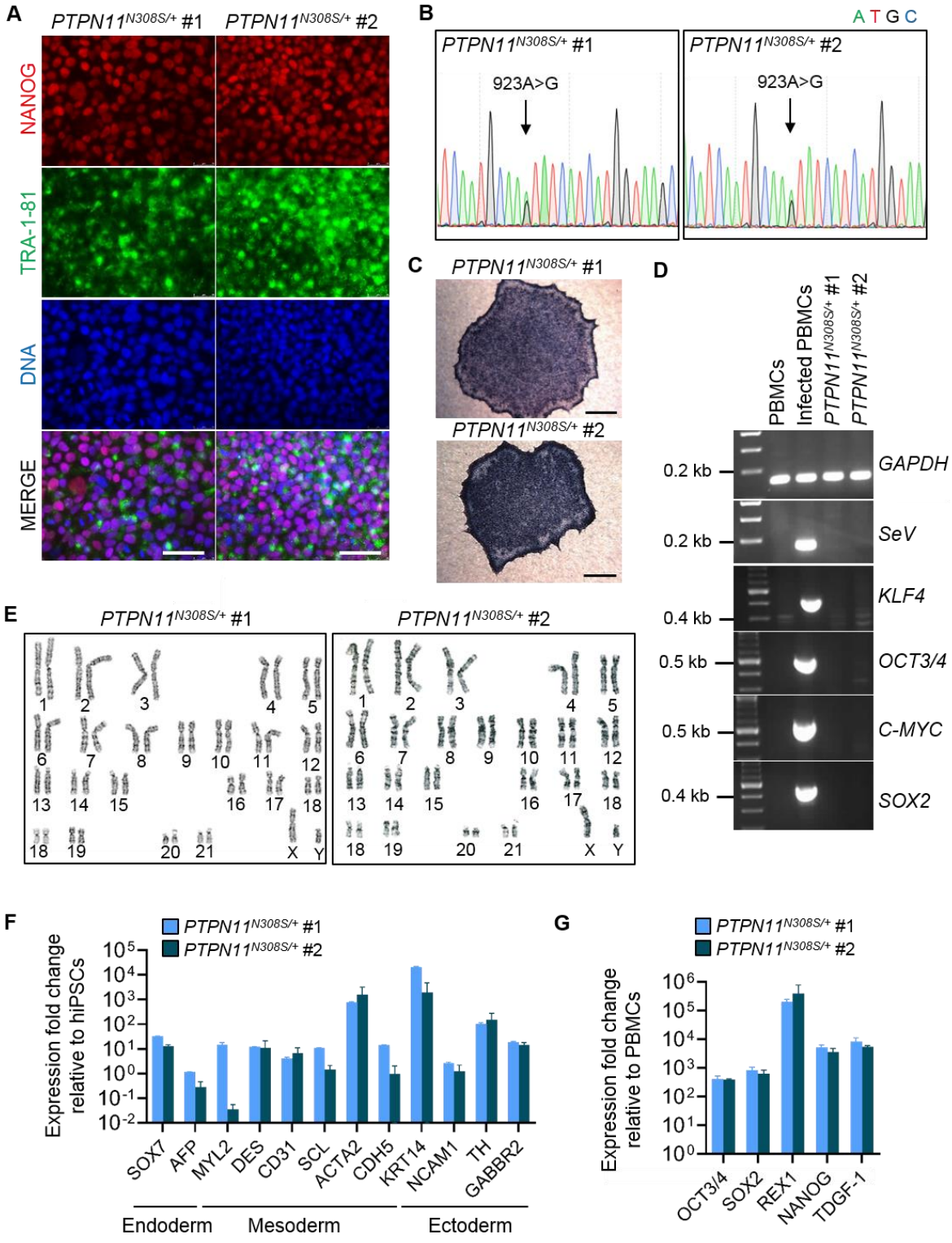

Figure S11. Generation of NS-CM patient-derived PTPN11N308S/+ iPSCs, Related to Figures 3 and 4. (A) Immunofluorescence analysis of the pluripotency markers Nanog and TRA-1-81 in *PTPN11*$^{N308S/+}$ iPSCs (#1: passage 18; #2: passage 20). Scale bar = 50 µm. **(B)** Sanger sequencing results of *PTPN11*$^{N308S/+}$ iPSCs confirming the presence of the heterozygous c.923A>G mutation in exon 8 of the *PTPN11* gene in both clones used in experiments (#1 and #2). **(C)** Bright field image of alkaline phosphatase staining performed on *PTPN11*$^{N308S/+}$ iPSC colonies (#1 and #2 both passage 6). Scale bar = 100 µm. **(D)** RT-PCR analysis of the Sendai vector and viral transgenes *OCT4*, *SOX2*, *KLF4* and *c-MYC* in uninfected peripheral blood mononuclear cells (PBMCs, negative control), Sendai-infected PBMCs (positive control) and *PTPN11*$^{N308S/+}$ iPSCs, using *GAPDH* as an endogenous control (#1: passage 15; #2: passage 14). **(E)** Normal karyotype confirmed in *PTPN11*$^{N308S/+}$ iPSCs (#1: passage

38, #2: passage 27). **(F)** qRT-PCR analysis of markers of endoderm (*SOX7*, *AFP*), mesoderm (*MYL2*, *CD31*, *DES*, *SCL*, *ACTA2*, *CDH5*) and ectoderm (*KRT14*, *NCAM1*, *TH*, *GABRR2*) using GAPDH as an endogenous control after 21 days of spontaneous EB differentiation of *PTPN11*$^{N308S/+}$ iPSCs (#1: passage 25; #2: passage 22). The mean expression fold change relative to iPSCs is indicated as mean ± SD, N = 2 differentiations. **(G)** qRT-PCR analysis of the pluripotency markers *OCT3/4*, *SOX2*, *NANOG*, *REX1* and *TDGF-1* using *GAPDH* as an endogenous control in *PTPN11*$^{N308S/+}$ iPSCs (#1: passage 15; #2: passage 14). The mean expression fold change relative to parental patient PBMCs is indicated as mean ± SD, N = 2 differentiations.

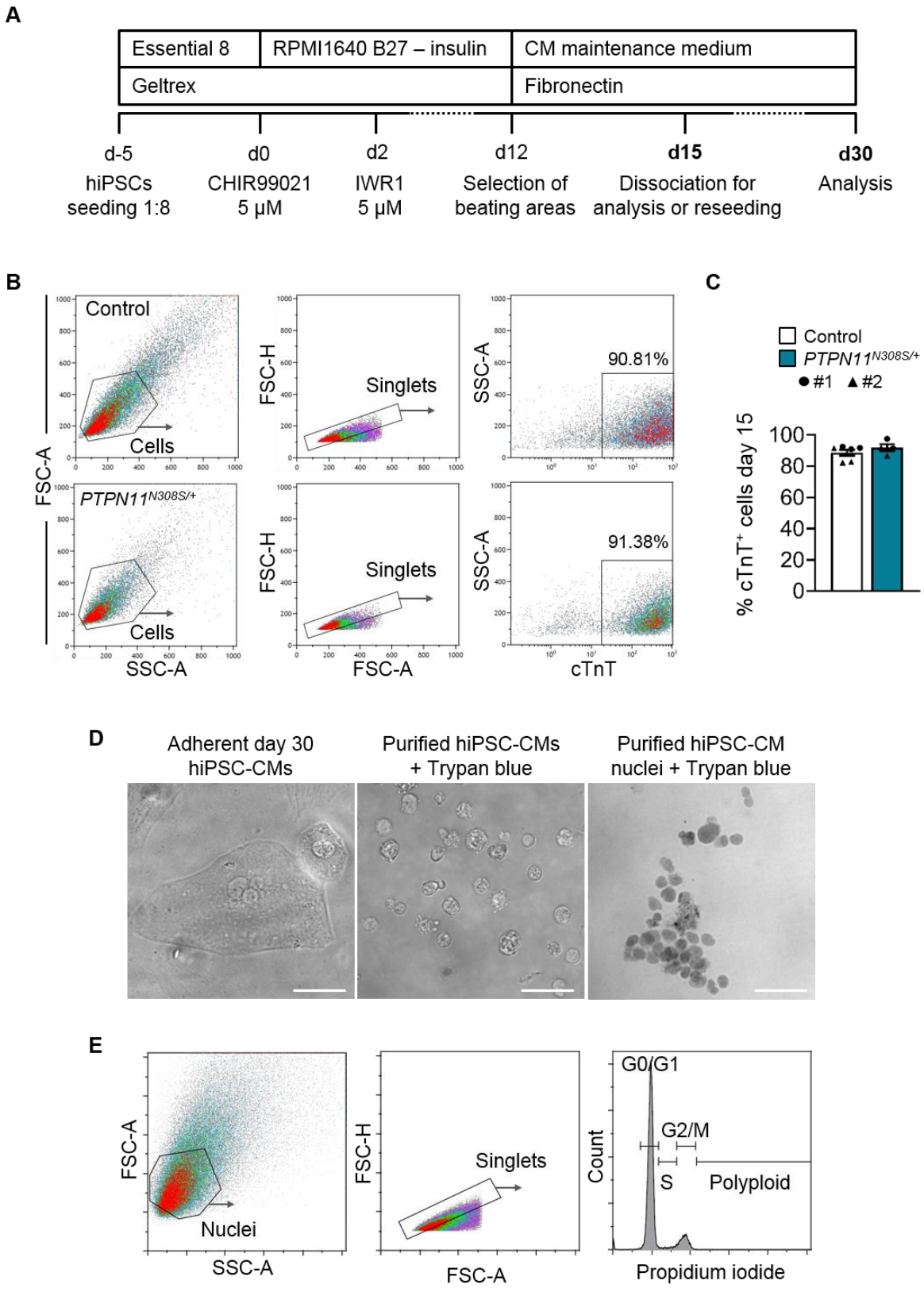

Figure S12. Differentiation of iPSCs into cardiomyocytes and isolation of iPSC-CM nuclei for DNA content analysis, Related to STAR Methods and Figures 3 and 4. (A) Graphical representation of the protocol used to differentiate iPSCs into cardiomyocytes (CMs) including media, basement coating and growth factors. Unless otherwise specified, iPSC-CMs were dissociated to single cells with papain and seeded at 25,000 cells/cm² at day 15 before analysis at day 30. **(B,C)** The efficiency of cardiac differentiation of control and *PTPN11*$^{N308S/+}$ iPSCs was assessed by flow cytometry analysis of cardiac troponin T (cTnT) in single cells (B). The percentage of cTnT^{+} cells obtained at day 15 is indicated as

mean ± SEM. Control #1 and #2 both N = 3 differentiations; *PTPN11*$^{N308S/+}$ #1 and #2 both N = 2 differentiations (C). FSC-A = forward scatter area, SSC-A = sideward scatter area, FSC-H = forward scatter height. **(D,E)** Representative images of day 30 iPSC-CMs before and after papain dissociation, purification and nuclei extraction. Trypan blue staining was used to verify nuclei yield and integrity (D). Gating strategy for the flow cytometry analysis of nuclei stained with propidium iodide to determine DNA content (G0/G1 phase: 2n; S phase: 2-4n; G2/M: 4n, polyploid: > 4n) (E). Scale bar in (D) = 50 µm.

Table S1. Clinical data of the NS-CM patients included in this study, Related to Figures 1 and 2

	Patient 1	**Patient 2**	**Patient 3**	**Patient 4**	**Patient 5**	**Patient 6**	**Patient 7**	**Patient 8**
Molecular genetic diagnosis								
Affected gene	*RAF1*	*RAF1*	*RAF1*	*PTPN11*	*PTPN11*	*RAF1*	*PTPN11*	*RAF1*
Nucleotide change	c.781C>T	c.770C>T	c.775T>A	c.1391G>C	c.923A>G	c.770C>T	c.922A>G	c.775T>A
Amino acid change	p.Pro261Ser	p.Ser257Leu	p.Ser259Thr	p.Gly464Ala	p.Asn308Ser	p.Ser257Leu	p.Asn308Asp	p.Ser259Thr
Gender	male	female	male	female	male	female	male	female
Age at diagnosis (months)	early perinatal period	early perinatal period	early perinatal period	early perinatal period	early perinatal period	early perinatal period	24	early perinatal period
Age at death (months)	na	na	na	na	na	na	na	15
Clinical characteristics and cardiac pathology at the time of surgery								
Age at surgery (months)	165	12	11	13	2	34	182	12
Ross classification	III	III	IV	III	IV	I	II	I
Medications	none	beta-blocker (4.3 mg/kg/day)	beta-blocker (11.1 mg/kg/day); diuretics	beta-blocker (1.1 mg/kg/day);	none	beta-blocker (3.43 mg/kg/day);	none	beta-blocker (9 mg/kg/day); disopyramid
TTE IVSd max (z-score)	9.7	5.6	6.22	7.87	5.2	4.96	5.05	6.7
TTE LVPWd max (z-score)	9.2	5.95	5.94	6.19	7.3	4.88	4.9	7.1
TTE LVEDd (z-score)	0.5	-6.4	-3.4	-4.9	-4.8	-0.5	-2.4	-3.1
LVOTO	yes	yes	yes	yes	Yes	yes	yes	yes
TTE peak LVOT gradient (mmHg)	130	75	130	72	85	92	105	140
RVOTO	yes	no	no	Yes	no	no	no	yes
TTE peak RVOT gradient (mmHg)	70	na	na	83	na	na	Na	36
TTE EF (%)	74	93	95	80	78	98	68	86
Dilated left atrium	no	no	yes	no	yes	no	no	yes
Mitral valve regurgitation	moderate	mild	moderate	No	mild	moderate	no	moderate
Arrhythmias	no	no	no	no	no	no	no	no
Histology								
Fibrosis	diffuse, 14%	diffuse and patchy, 11%	diffuse, 3%	diffuse and patchy, 6%	focal, 2%	na	diffuse, 3%	na

Myocyte disarray	severe	mild	mild	severe	moderate	na	mild	na
Cardiac pathology at the time of last follow-up								
Age at last follow-up (months)	184	101	96	na	109	78	220	na
Ross classification	II	II	I	na	I	I	II	na
Medications	beta-blocker (0.8 mg/kg/day); diuretics; Amiodaron	beta-blocker (14 mg/kg/day), disopyramide	beta-blocker (13 mg/kg/day), disopyramide	na	none	none	bisoprolol (0.12 mg/kg/day)	na
TTE IVSd max (z-score)	8.4	6.1	7.8	na	0.15	3.6	5.1	na
TTE LVPWd max (z-score)	6.5	6.5	6.4	na	1.4	3.0	2.5	na
TTE LVEDd (z-score)	-1.2	-3.1	-9.1	na	-1.9	-5.1	0.8	na
LVOTO	no	yes	no	na	no	no	yes	na
TTE peak LVOT gradient (mmHg)	na	40	na	na	na	na	30	na
RVOTO	yes	no	no	na	no	no	no	na
TTE peak RVOT gradient (mmHg)	35	na	na	na	na	na	na	na
TTE EF (%)	78	89	92	na	70	72	70	na
Dilated left atrium	yes	yes	no	na	no	no	no	na
Mitral valve regurgitation	moderate	no	no	na	no	no	no	na
Arrhythmias	yes	no	no	na	no	no	no	na
Clinical course	no further intervention	second surgical septal myectomy at 63 months of age	right ventricular outflow tract resection at 96 months of age	lost to follow-up	second surgical septal myectomy at 76 months of age	no further intervention	no further intervention	passed away from necrotizing enterocolitis, sepsis, and multiorgan failure after surgical septal myectomy at 15 months of age

na: not applicable / not available; TTE: transthoracic echocardiography; IVSd: enddiastolic interventricular septal thickness; LVPWd: enddiastolic left ventricular posterior wall thickness; LVEDd: enddiastolic left ventricular diameter; LVOTO: left ventricular outflow tract obstruction; RVOTO; right ventricular outflow tract obstruction; EF: ejection fraction;

Table S2. Characteristics of the LV myocardial tissue included in each assay, Related to Figures 1 and 2

Group	Affected gene	Genetic variant	Gender	Age at operation (years)	Assays
NS-CM	*RAF1*	p.Pro261Ser	male	13.75	Mant-ATP assay, Histopathology
	RAF1	p.Ser257Leu	female	1	Mant-ATP assay, Histopathology, RNA-Seq
	RAF1	p.Ser259Thr	male	0.9	Histopathology, RNA-Seq
	PTPN11	p.Gly464Ala	female	1.1	Mant-ATP assay, Histopathology
	PTPN11	p.Asn308Ser	male	0.2	Histopathology, RNA-Seq
	RAF1	p.Ser257Leu	female	2.8	RNA-Seq
	PTPN11	p.Asn308Asp	male	15.6	Mant-ATP assay, Histopathology, RNA-Seq
	RAF1	p.Ser259Thr	female	1	Mant-ATP assay
HCM	*MYH7*	p.R791W	female	40	Mant-ATP assay
	MYH7	p.R791Q	male	38	Mant-ATP assay
	MYBPC3	p.Leu1200Pro	male	16.1	Histopathology, RNA-Seq
	MYH7	p.Ile736Thr	male	10.5	RNA-Seq
	MYBPC3	p.Arg495Gln	male	2.5	Histopathology
	MYBPC3	ND	male	1.1	Histopathology
	MYH7	p.Arg403Trp	female	11.1	Histopathology
	Familial non-syndromic HCM (affected gene and variant unknown)		male	1.7	Histopathology
			female	7	Histopathology
Control (non-failing heart)	NA		female	42	Mant-ATP assay
			male	38	Mant-ATP assay
Control (transplanted hearts)	NA		female	5	Histopathology
			male	1.3	Histopathology
			male	3	Histopathology
			female	2	Histopathology
			male	1.75	Histopathology
			female	4	Histopathology
Control (VSD)	NA		male	0.5	RNA-Seq
			female	1.8	RNA-Seq
			male	3.3	RNA-Seq
			male	9.6	RNA-Seq

Table S4. Top 20 genes upregulated in NS-CM tissue, Related to Figure 2.
(Log2 fold change in NS-CM and HCM tissue compared to control)

Gene	Group	Log2 fold change vs CTRL	P value (< 0.05 in bold)
EREG	NS-CM	6.153	**0.01389**
	HCM	0.183	0.22345
CUX2	NS-CM	5.226	**0.01125**
	HCM	2.018	**0.00009**
FGF10	NS-CM	4.955	**0.01242**
	HCM	0.042	0.66659
MIR4701	NS-CM	4.831	**0.00469**
	HCM	0.083	0.65029
ATP1A4	NS-CM	4.029	**0.01127**
	HCM	1.107	**0.00088**
NBPF24	NS-CM	3.608	**0.04601**
	HCM	0.092	0.66895
NAT2	NS-CM	3.459	**0.02271**

	HCM	0.014	0.93911
GPR179	NS-CM	3.428	**0.04155**
	HCM	0.153	0.43051
LRRN4	NS-CM	3.296	**0.00994**
	HCM	0.197	0.37932
AK128707	NS-CM	3.173	**0.00048**
	HCM	0.336	0.22754
U4	NS-CM	3.160	**0.02679**
	HCM	-0.006	0.97074
SV2C	NS-CM	3.104	**0.00683**
	HCM	0.435	0.07454
AX747124	NS-CM	2.993	**0.03589**
	HCM	0.615	**0.04618**
SYTL5	NS-CM	2.987	**0.00096**
	HCM	1.363	**0.00001**
SMCR5	NS-CM	2.927	**0.00282**
	HCM	0.021	0.92410
AK124399	NS-CM	2.882	**0.03291**
	HCM	-0.133	0.64960
AK094909	NS-CM	2.777	**0.04208**
	HCM	0.146	0.45625
TMEM155	NS-CM	2.747	**0.00063**
	HCM	-0.495	0.10181
KRT80	NS-CM	2.687	**0.00768**
	HCM	0.498	0.10015
MIR4257	NS-CM	2.589	**0.03774**
	HCM	0.065	0.75557

Table S6. List of Antibodies, Related to STAR Methods

Target	**Host**	**Reference**	**Concentration**
Nanog	Rabbit	Abcam ab21624	1:500 (IF)
TRA-1-81	Mouse	BD Pharmingen 560174	1:20 (IF)
Sendai virus	Rabbit	MBL PD029	1:1000 (IF)
Cardiac troponin T	Mouse	Invitrogen MA5-12960	1:500 (IF)
Cardiac troponin T	Rabbit	Abcam ab92546	1:500 (IF)
Cardiac troponin T-VioBlue	Recombinant human	Miltenyi Biotec 130-120-402	1:50 (FC)
Plakophilin 2	Guinea pig	Origene AP09554SU-N	1:100 (IF)
Ki67	Mouse	BD Biosciences 556003	1:100 (IF)
α-actinin	Mouse	Sigma-Aldrich A7811	1:250 (IF)
Dystrophin	Rabbit	Zytomed 504-2664	1:1000 (IHC)
Anti-mouse IgG Alexa Fluor 647	Goat	Invitrogen A-21235	1:500 (IF)
Anti-guinea pig IgG Alexa Fluor A594	Goat	Invitrogen A-11076	1:500 (IF)
Anti-rabbit IgG Alexa Fluor A488	Goat	Invitrogen A-11008	1:500 (IF)

Table S7. List of Primer sequences, Related to STAR Methods

Name	Use	Sequence	
Sendai Virus	RT-PCR	Forward	5‘GGATCACTAGGTGATATCGAGC
		Reverse	5‘ACCAGACAAGAGTTTAAGAGATATGTATC
Hs Sox2 trans	RT-PCR	Forward	5‘ATGCACCGCTACGACGTGAGCGC
		Reverse	5‘AATGTATCGAAGGTGCTCAA
Hs Klf4 trans	RT-PCR	Forward	5‘TTCCTGCATGCCAGAGGAGCCC
		Reverse	5‘AATGTATCGAAGGTGCTCAA
Hs c-Myc trans	RT-PCR	Forward	5‘TAACTGACTAGCAGGCTTGTCG
		Reverse	5‘AATGTATCGAAGGTGCTCAA
Hs Oct3/4 trans	RT-PCR	Forward	5‘CCCGAAAGAGAAAGCGAACCAG
		Reverse	5‘AATGTATCGAAGGTGCTCAA
Hs ACTA2	qPCR	Forward	5‘GTGATCACCATCGGAAATGAA
		Reverse	5‘TCATGATGCTGTTGTAGGTGGT
Hs AFP	qPCR	Forward	5‘GTGCCAAGCTCAGGGTGTAG
		Reverse	5‘CAGCCTCAAGTTGTTCCTCTG
Hs CD31	qPCR	Forward	5‘ATGCCGTGGAAAGCAGATAC
		Reverse	5‘CTGTTCTTCTCGGAACATGGA
Hs CDH5	qPCR	Forward	5‘CCTACCAGCCCAAAGTGTGT
		Reverse	5‘TGTCCTTGTCTATTGCGGAGA
Hs DES	qPCR	Forward	5‘GTGAAGATGGCCCTGGATGT
		Reverse	5‘TGGTTTCTCGGAAGTTGAGG
Hs GABRR2	qPCR	Forward	5‘CTGTGCCTGCCAGAGTTTCA
		Reverse	5‘ACGGCCTTGACGTAGGAGA
Hs GAPDH	qPCR	Forward	5‘TCCTCTGACTTCAACAGCGA
		Reverse	5‘GGGTCTTACTCCTTGGAGGC
Hs GATA4	qPCR	Forward	5‘GGCCTGTCATCTCACTACGG
		Reverse	5‘ATGGCCAGACATCGCACT
Hs KRT14	qPCR	Forward	5‘CACCTCTCCTCCTCCCAGTT
		Reverse	5‘ATGACCTTGGTGCGGATTT
Hs MYH6	qPCR	Forward	5‘TCAGGATTCTCCGTGAAGGG
		Reverse	5‘CTCTTCCTTGTCATCGGGCA
Hs MYH7	qPCR	Forward	5’TGTAGACACACTTGAGTAGCCC
		Reverse	5‘ACGGTCACTGTCTTGCCATA

Hs NANOG	qPCR	Forward	5‘TGCAAGAACTCTCCAACATCCT
		Reverse	5‘ATTGCTATTCTTCGGCCAGTT
Hs NCAM1	qPCR	Forward	5‘CGACCATCCACCTCAAAGTC
		Reverse	5‘CCATGGCAGTCTGGTTCTCT
Hs OCT4	qPCR	Forward	5‘GACAGGGGGAGGGGAGGAGCTAGG
		Reverse	5‘CTTCCCTCCAACCAGTTGCCCCAAAC
Hs REX1	qPCR	Forward	5‘ACCAGCACACTAGGCAAACC
		Reverse	5‘TTCTGTTCACACAGGCTCCA
Hs SCL	qPCR	Forward	5‘CCAACAATCGAGTGAAGAGGA
		Reverse	5‘CCGGCTGTTGGTGAAGATAC
Hs SOX2	qPCR	Forward	5‘GGGAAATGGGAGGGGTGCAAAAGAGG
		Reverse	5‘TTGCGTGAGTGTGGATGGGATTGGTG
Hs SOX7	qPCR	Forward	5‘TGAACGCCTTCATGGTTTG
		Reverse	5‘AGCGCCTTCCACGACTTT
Hs TH	qPCR	Forward	5‘TGTACTGGTTCACGGTGGAGT
		Reverse	5‘TCTCAGGCTCCTCAGACAGG
Hs TDGF-1	qPCR	Forward	5‘CCCAAGAAGTGTTCCCTGTG
		Reverse	5‘ACGTGCAGACGGTGGTAGTT
Hs TNNT2	qPCR	Forward	5‘AGCATCTATAACTTGGAGGCAGAG
		Reverse	5‘TGGAGACTTTCTGGTTATCGTTG